Accepted Manuscript

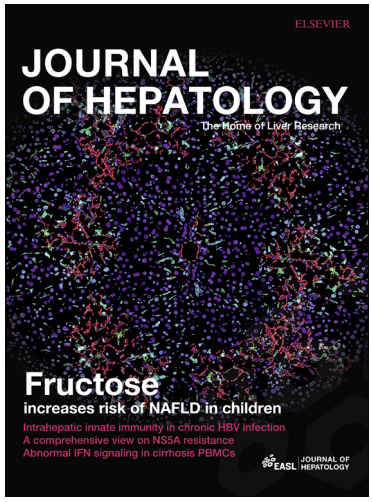

hiPSC hepatocyte model demonstrates the role of unfolded protein response and inflammatory networks in α_1-antitrypsin deficiency

Charis-Patricia Segeritz, Sheikh Tamir Rashid, Miguel Cardoso de Brito, Maria Serra Paola, Adriana Ordonez, Carola Maria Morell, Joseph E. Kaserman, Pedro Madrigal, Nicholas Hannan, Laurent Gatto, Lu Tan, Andrew A. Wilson, Kathryn Lilley, Stefan J. Marciniak, Bibekbrata Gooptu, David A. Lomas, Ludovic Vallier

PII: S0168-8278(18)32113-5
DOI: https://doi.org/10.1016/j.jhep.2018.05.028
Reference: JHEPAT 6990

To appear in: *Journal of Hepatology*

Received Date: 6 October 2017
Revised Date: 25 April 2018
Accepted Date: 17 May 2018

Please cite this article as: Segeritz, C-P., Rashid, S.T., Cardoso de Brito, M., Paola, M.S., Ordonez, A., Morell, C.M., Kaserman, J.E., Madrigal, P., Hannan, N., Gatto, L., Tan, L., Wilson, A.A., Lilley, K., Marciniak, S.J., Gooptu, B., Lomas, D.A., Vallier, L., hiPSC hepatocyte model demonstrates the role of unfolded protein response and inflammatory networks in α_1-antitrypsin deficiency, *Journal of Hepatology* (2018), doi: https://doi.org/10.1016/j.jhep.2018.05.028

hiPSC hepatocyte model demonstrates the role of unfolded protein response and inflammatory networks in α_1-antitrypsin deficiency

Charis-Patricia Segeritz*[1,2], Sheikh Tamir Rashid*[1,2,3], Miguel Cardoso de Brito[1], Maria Serra Paola[3], Adriana Ordonez[2], Carola Maria Morell[1], Joseph E. Kaserman[5], Pedro Madrigal[1], Nicholas Hannan[1], Laurent Gatto[6], Lu Tan[2], Andrew A. Wilson[5], Kathryn Lilley[6], Stefan J. Marciniak[2], Bibekbrata Gooptu[2,3], David A. Lomas^[4], Ludovic Vallier^[1,7]

Joint * first authors and ^ last authors.

[1] Wellcome Trust and MRC Cambridge Stem Cell Institute, Department of Surgery, University of Cambridge, UK.

[2] Cambridge Institute for Medical Research, University of Cambridge, UK.

[3] Centre for stem cells and regenerative medicine & Institute for Liver Studies, King's College London, UK

[4] UCL Respiratory, University College London, UK

[5] Center for Regenerative Medicine (CReM) of Boston University and Boston Medical Center, Boston, MA 02118, USA

[6] Cambridge Centre for Proteomics, Department of Biochemistry, University of Cambridge, Building O, Downing Site, Cambridge CB2 1QW, UK.

[7] Wellcome Trust Sanger Institute, Genome Campus Hinxton, UK.

Address for correspondence UCL Respiratory Biology: d.lomas@ucl.ac.uk

Address for correspondence Cambridge Stem Cell Institute: lv225@cam.ac.uk

Address for correspondence King's Liver Institute: tamir.rashid@kcl.ac.uk

KEYWORDS:

Hepatocyte, inherited liver disease, human induced pluripotent stem cell, α_1-antitrypsin deficiency, inflammation.

ELECTRONIC WORD COUNT: 6000 (including abstract)

NUMBER OF FIGURES AND TABLES: 6 Figures.

CONFLICT OF INTEREST STATEMENT:

STR and LV are scientific founders of Definigen Ltd. (shares and consultancy). DAL is working with GlaxoSmithKline to develop small molecules that block the intracellular polymerisation of α_1-antitrypsin. For all other authors, conflicts of interest: none.

FINANCIAL SUPPORT STATEMENT:

CPS is funded through a Children's Liver Disease Foundation (CLDF) studentship. DAL is funded by the Medical Research Council, Wellcome Trust, GlaxoSmithKline, the Rosetrees Trust, EPSRC and UCLH NIHR Biomedical Research Centre. LV, PM, MCB, NH are funded by ERC Relieve-IMDs and ERC advanced grant New-Chol, Cambridge University Hospitals National Institute for Health Research Biomedical Research Center, and the core support grant from the Wellcome Trust and Medical Research Council to the Wellcome Trust – Medical Research Council Cambridge Stem Cell Institute. STR is funded by an MRC Clinician Scientist Fellowship award.

AUTHOR CONTRIBUTIONS:

STR, DAL and LV conceived the project. CPS led the experimental procedures with support from all other co-authors. CPS, STR, DAL and LV analysed the data and wrote the manuscript.

ABSTRACT (257 words)**:**

Background and Aims: α_1-antitrypsin deficiency (A1ATD) is an autosomal recessive disorder caused by mutations in the *SERPINA1* gene. Individuals with the Z variant (Gly342Lys) retain polymerised protein in the endoplasmic reticulum (ER) of their hepatocytes, predisposing them to liver disease. The concomitant lack of circulating A1AT also causes lung emphysema. Greater insight into the mechanisms that link protein misfolding to liver injury will facilitate the design of novel therapies.

Methods: hiPSC-derived hepatocytes provide a novel approach to interrogate the molecular mechanisms of A1ATD because of their patient-specific genetic architecture and reflection of human physiology. To that end, we utilised patient-specific hiPSC hepatocytes (ZZ-HLCs) derived from an A1ATD (ZZ) patient, which faithfully recapitulated key aspects of the disease at the molecular and cellular level. Subsequent functional and "omics" comparisons of these cells with their genetically corrected isogenic-line (RR-HLCs) and primary hepatocytes/human tissue allowed the identification of new molecular markers and disease signatures.

Results: Our studies showed that abnormal A1AT polymer processing (immobilized ER components, reduced luminal protein mobility and disrupted ER cisternae) occurred heterogeneously within hepatocyte populations and

was associated with disrupted mitochondrial structure, presence of the oncogenic protein AKR1B10 and two upregulated molecular clusters centred on members of inflammatory (IL-18 and Caspase-4) and unfolded protein response (Calnexin and Calreticulin) pathways. These results were validated in a second patient-specific hiPSC line.

Conclusions: Our data identified novel pathways that potentially link the expression of Z A1AT polymers to liver disease. These findings could help pave the way towards identification of new therapeutic targets for treatment of A1ATD.

LAY SUMMARY:

This study compared the gene expression and protein profiles of healthy liver cells and those affected by the inherited disease α_1-antitrypsin deficiency. This approach identified specific factors primarily present in diseased samples which could provide new targets for drug development. This study also demonstrates the interest of using hepatic cells generated from human induced pluripotent stem cells to model liver disease *in vitro* for uncovering new mechanisms with clinical relevance.

GRAPHICAL ABSTRACT: Attached

HIGHLIGHTS:

- Modelling α_1-antitrypsin deficiency liver disease using hiPSC-derived hepatocytes reveals disruption of the endoplasmic reticulum into isolated cisternae.

- Comparative transcriptomic and proteomics between diseased hiPSC-derived hepatocytes and their isogenic wildtype provides insights into disease mechanisms.
- AKR1B10 was identified as a putative biomarker for α_1-antitrypsin deficiency.

INTRODUCTION:

α_1-antitrypsin (A1AT) is a 52 kDa protein encoded by the *SERPINA1* gene synthesized primarily by hepatocytes [1]. Secreted into the blood stream, it acts to control the function of neutrophil elastase, particularly in the lung [2]. A1AT also exerts anti-apoptotic and anti-inflammatory properties during inflammation and hepatic injury. Most people carry the wildtype M allele, while the rarer Z variant (found in 1-3% of the population), is associated with the most common and severe form of clinically significant A1AT deficiency (A1ATD) [3]. The Z allele is caused by a Glu342Lys mutation in exon 5 of the *SERPINA1* gene, leading to conformational instability within the protein [4]. Approximately 70 % of synthesized Z A1AT is degraded by intracellular quality control mechanisms, 15 % is secreted whilst the remaining 15 % accumulates in hepatocytes as ordered polymers. These polymers are associated with neonatal hepatitis, cirrhosis and hepatocellular carcinoma. Furthermore, the significant reduction in circulating plasma A1AT levels leads to uncontrolled proteolytic activity within the lung and development of early onset panlobular emphysema [5].

Despite the recognition of A1ATD over fifty years ago [6], the detailed molecular mechanisms linking A1AT polymer accumulation to the

development of liver disease remain poorly understood. This has been hampered by the availability of primary human hepatocytes expressing wildtype and mutant forms of A1AT capable of surviving in culture long-term. Although the use of animal models and artificial A1AT-expressing cell systems have contributed significantly to improved understanding of the disease processes [7] [8] [9], multiple gene copies, interference of endogenous animal antiproteases, lack of pathological features post-polymer accumulation, and the absence of endogenous promoters to activate gene expression represent challenges for translating new findings in these model systems to man.

The advent of human induced pluripotent stem cells (hiPSCs) [10] has provided an exciting platform to address these obstacles. Indeed, PiZZ hiPSCs (ZZ-hiPSCs) derived from patients with A1ATD were shown to differentiate into hepatocyte-like cells (ZZ-HLCs) that recapitulate the modified post-translational processing and secretion kinetics of mutant A1AT [11] [12]. Furthermore, patient-specific HLCs were genetically corrected to erase the disease signature (RR-HLCs) [13] and so generated a perfect control cell line with which to perform mechanistic studies.

Using these tools, we first established the suitability of HLCs to study the mechanisms of A1ATD by benchmarking their gene expression, protein synthesis and metabolic activity against primary hepatocytes. Then, by comparing the transcriptome and ER-enriched proteome of ZZ- and RR-HLCs, we validated the platform's efficiency for identifying novel biomarkers and pathways involved in mediating the disease processes that may be of immediate clinical relevance.

MATERIALS AND METHODS:

hiPSC culture and hepatic differentiation

All hiPSC lines used in this study have were derived as previously described [11] under Addenbrooke's Hospital Ethics reference number 08/H0311/201; R&D No. A091485. These cells were maintained at 37 ℃ in humidified incubators supplemented with 5 % v/v carbon dioxide and were differentiated using our established hepatic differentiation protocol with minor modifications [14]: Cells were differentiated at 5 % oxygen and two splitting steps allowed for scale-up and prolonged maturation of differentiating cells (Supplementary Fig. 1A). During the splitting steps on day 8 and day 25, cells were washed with PBS and dissociated with TrypLE^{TM} (Life Technologies, 12563-029) for 20-45 min at 37 ℃. Harvested cells were centrifuged at 100 x g for 3 min. Cells were resuspended in RPMI (day 8 split) or HepatoZYME-SFM (day 25) (Thermo Fisher, 17705-021). Cells were counted and resuspended in RPMI and Activin (day 8 split) or HepatoZYME-SFM (Thermo Fisher, 17705-021), OSM and HGF (day 25 split), supplemented in each case with ROCK inhibitor (1 µL/mL) to a concentration of 210,500 cells/cm^2.

Primary hepatocyte procurement

Commercially plated human primary hepatocytes from two donors were purchased from Biopredic International (France). The cells exhibited viabilities between 88-93% after isolation, fulfilled the manufacturer's requirements of Phase I and II-dependent enzyme activities and were cultured for 48 h in hepatocyte medium prior to harvesting. Fresh human primary hepatocytes were kindly provided by Dr. Roque Bort with approval of the hospital's ethics

committee (Instituto de Investigación Sanitaria La Fe, Valencia, Spain). Upon isolation, hepatocytes were snap frozen and the resulting cell pellets were directly lysed for RNA extraction.

RNA-seq

Library preparation of RNA samples were performed with the Illumina TruSeq RNA Sample Preparation V2 assay. Samples were multiplexed on two lanes with 40 bp (HLCs) or 75bp (PiZZ/PiMM) read lengths, single strand and single-end (HLCs) or paired-end (PiZZ/PiMM) reads and generated ~16.5 million reads per sample on the Illumina HiSeq 2000. Bioinformatic analysis were carried out following standard procedures [11] and of raw data are available on arrayexpress accession number E-MTAB-6781.

RESULTS:

hiPSC-derived hepatocyte-like cells are suitable for modelling human disease

We have previously generated disease specific hiPSCs (ZZ-hiPSCs) [11] and created an isogenic wildtype line (RR-hiPSC) using genome editing [13]. Once differentiated, ZZ-derived hepatocyte like cells (ZZ-HLC) displayed intracellular polymer retention whilst corrected cells (RR-HLC) secreted normal levels of A1AT. Thus, RR-HLC represent the ideal control for molecular studies since phenotypic differences observed between both cell types should exclusively be attributable to the misfolding of mutant A1AT in HLC-ZZs and not to variability between hiPSCs lines of different genetic backgrounds [15]. To further validate this hypothesis, we compared the

hepatic function of ZZ-HLCs and RR-HLCs using as positive control primary hepatocytes freshly isolated, cryopreserved or freshly plated. Of note, we applied an optimised protocol [14] allowing HLCs to differentiate for an extended period of time and thus to increase their functional repertoire (Supplementary Fig. 1A-C). As expected, HLCs expressed a diversity of hepatic markers including *A1AT*, *ALB* and *HNF4α* at levels equivalent to primary hepatocytes (Fig. 1A-C). They also displayed *CYP3A4* expression and activity although at significantly lower levels than primary cells (Fig. 1A, Supplementary Fig. 1B). Reversely, HLCs showed expression of foetal markers *CYP3A7* and *AFP* at higher levels (Fig. 1A) thereby confirming their foetal identity [16]. More importantly, ZZ-HLCs and RR-HLCs expressed comparable levels of hepatic markers (Fig. 1A). These observations were confirmed by immunostaining and DELFIA, showing these markers to be expressed at equivalent levels in both cell types with the exception of A1AT, which was synthesised in lower concentrations into ZZ-HLCs culture media (Fig. 1B-C). To confirm this observation, A1AT trafficking in ZZ-HLCs was assessed by growing HLCs in the presence of radioactively labelled [^{35}S] Cys/Met and by subsequently tracking its transition from the intracellular to the extracellular space over the course of four hours. The band intensities of these pulse-chase experiments revealed a slower rate of glycoprotein maturation (e.g. sialic acid residue incorporation) and trafficking of A1AT to the extracellular space in ZZ-HLCs (Fig. 1D). Whilst wildtype A1AT was almost fully secreted after four hours in RR-HLCs, mutant A1AT in ZZ-HLCs was mostly degraded or retained intracellularly during the same time period [17]. Taken together, these results demonstrate that ZZ-HLCs and RR-HLCs

have reproducible biological characteristics *in vitro* except for the processing of A1AT and therefore provide a suitable control-study pair for in-depth characterisation of the disease pathophysiology of A1ATD.

ZZ-HLCs abnormally process A1AT polymer in a heterogenous, ER-dependent manner

To investigate the impact of A1AT protein accumulation on cellular trafficking, we studied the hepatic endoplasmic reticulum (ER) – the site at which mutant A1AT proteins aggregate – at a single cell level. ZZ- and RR-HLCs were transfected with the ER marker GFP-KDEL that has been shown to co-localise with A1AT polymers [9]. Transfections of HLCs with the GFP-KDEL construct yielded a population of RR-HLCs which all contained normal, reticular ER morphologies (Fig. 2A). In contrast, ZZ-HLCs frequently displayed large ER inclusions. We classified these as inclusions of small, medium or large size and quantified the percentage of cells containing each sub-type (Fig. 2B). Overall, 40 % of ZZ-HLCs showed inclusions, whilst the remaining 60 % of cells exhibited a normal ER. We next assessed for the effect of intracellular inclusions on ER architecture using “Fluorescence Loss In Photobleaching” (FLIP) and “Fluorescence Recovery After Photobleaching” (FRAP) to track live, GFP-KDEL transfected ZZ-HLCs and RR-HLCs [18]. This allowed an evaluation of the cell’s ER connectivity (FLIP) and luminal protein mobility (FRAP) by monitoring the diffusion rates of inert fluorescent probes throughout different ER morphologies. Repeated photobleaching of a pre-defined fluorescent region resulted in complete depletion of fluorescence in inclusion-free ZZ- and RR-HLCs, while neighbouring cells were unaffected (Fig. 3A). Of

particular note was the small, consistent recovery of fluorescence in between the bleaching events, suggesting rapid diffusion of unbleached KDEL-fluorophores back to the area of interest. These observations reinforced our previous results obtained on transformed cell lines [19] by showing that in wildtype HLCs, ER proteins can sample distant compartments of the ER by diffusion when enclosed by connected, tubular ER luminae. In contrast, in inclusion-bearing ZZ-HLCs, FLIP within large inclusions resulted in the localised loss of KDEL-GFP fluorescence with no recovery of fluorescence after bleaching events. Furthermore, neighbouring inclusions were not affected, indicating walled-off ER cisternae with no or restricted ability for protein diffusion or interactions between them. These observations were further confirmed using another fluorescent protein chimera, the cytoplasmic domain of an ER signal anchor membrane protein (CytERM) [20]. FLIP performed on ZZ-HLCs with large inclusions transfected with fluorescent CytERM resulted in complete loss of fluorescence of the inclusion's ER membrane, whilst neighbouring inclusions were unaffected (Fig 3B). Finally, fragmentation and isolation of ER inclusions were confirmed using Z-stack images captured across ZZ-HLCs transfected with the fluorescent ER membrane protein (Fig. 3C). The mobility of ER proteins was then quantified using FRAP assays [18]. The pre-bleach fluorescence level of a selected region of interest inside the cytoplasm was normalised to 100% and a single bleaching event was performed within the region of interest. Diffusion rates of unbleached KDEL-GFP molecules from adjacent areas into the bleached region were determined by monitoring the restoration of fluorescent levels into the region of interest. We observed that the patterns of fluorescent recovery

were similar within regions of reticular ER in RR- and ZZ-HLCs (Fig. 4A). Mapping the percentage of fluorescent rescue to the area of bleach showed almost immediate recovery at approximately 60 %, which was further restored to nearly 90 % in RR-HLCs. In contrast, inclusion-bearing ZZ-HLCs showed recovery of only 30-40 % of the original KDEL-GFP fluorescence. Regression analysis to reveal the rates of recovery, i.e. the slope of the respective fluorescent recovery curves, confirmed faster diffusion rates of proteins in areas of connected reticular ER compared to that seen in areas with disrupted ER morphologies (RR-HLC: 2.92 ± 0.75, ZZ-HLC no inclusions: 3.99 ± 1.03, ZZ-HLC with inclusions 1.23 ± 0.22). There appeared no or very small recovery of fluorescence in bleaching of larger inclusions, suggesting a size-dependent isolation of inclusions (Fig. 4B). To quantify the percentage of total fluorescent molecules that contribute to the fluorescent recovery of the photobleached area during the assayed time frame, we assessed the mobile fractions associated with individual ER morphologies. These showed that protein viscosities of reticular ER morphologies were significantly lower than that of fractionated ER sites ($p \leq 0.0001$) (Fig. 4C). In summary, these data showed that polymer accumulation in A1ATD reduced ER protein diffusion rates suggestive of immobilised ER components, reduced protein mobilities and/or disrupted ER cisternae in inclusion-bearing ZZ-HLCs [21].

Transcriptome and proteome analyses suggest ZZ-HLCs acquire mitochondrial abnormalities and are poised for malignancy

Given the abnormalities in protein mobility observed in the ER, we hypothesised that polymer accumulation in ER inclusions could be associated

with specific proteins inhibiting A1AT polymer degradation and eliciting stress responses [22] [23] [24]. To investigate this hypothesis, we performed proteomic analyses on ER fractions isolated from ZZ- and RR-HLCs (Fig. 5A). Three independent batches of ZZ- and RR-HLCs were fractionated into their subcellular ER fractions and analysed by label-free mass spectrometry. We identified 2683 unique proteins in the ZZ- and RR-HLC ER proteomes, which were enriched most significantly for the ER (adjusted p-value: 7.1^{-91}) and mitochondria (adjusted p-value: 1.6^{-172}). Among these proteins, 14 were exclusively identified in all three batches of ZZ-HLCs whilst 3 proteins were present only in the RR-HLCs (Fig. 5B). By GO Enrichment Analysis, these 17 proteins with strict distribution patterns displayed a diversity of functions involved in intracellular trafficking, extracellular matrix organization and enzymatic activity. Five of these proteins (29%) were attributed to mitochondrial localization and oxidoreductase activity: GLUD2, GFER, OXCT1, EARS2 and ADCK3. In order to further understand the implications of A1AT protein accumulation on a whole-cell scale, genome-wide RNA sequencing (RNA-seq) was performed on ZZ-HLCs and RR-HLCs. Statistical analysis revealed 1675 genes with significantly different expression (false-discovery rate (FDR) <5 %), the majority of which were protein-coding genes (93.4 %) (Fig. 5C). Of the 1675 differentially expressed genes, 959 were upregulated in ZZ-HLCs (958 of them with a fold change >1.5), while 716 genes were downregulated in ZZ-HLCs (715 of them with a fold change <-1.5). 319 genes with differential transcript expression were also detected in the mass-spectrometry dataset (Fig. 5D). We then combined both proteomic and transcriptomic data sets by considering differential abundances of

proteins and genes with log-fold changes >2 or <-2. Candidate markers that fulfilled these parameters included 18 upregulated and 15 downregulated genes/proteins (Fig. 5E), of which 15 % were ER-localised proteins (CLGN, KDELR3, COL4A1, COL14A1, CYP1A1). Of note, the low correlation of data points seen under these conditions may be explained by the comparison of whole-cell transcriptomes with subcellular ER-specific proteomes. We next focused on examining the absolute gene expression of the assayed genes and considering ZZ-HLCs as the reference. We found that 20 of the 21 most highly-expressed and differentially upregulated genes in ZZ-HLCs were of mitochondrial origin (Fig. 5F). The majority of their functional repertoire was relevant to oxidoreductase activity and mitochondrial ATP synthesis in the electron transport chain and included NADH dehydrogenases, ATP synthases, cytochromes b and c. The only non-mitochondrial gene in the very highly-expressed, upregulated gene cluster was fibrinogen gamma chain (*FGG*), upregulation of which has previously been associated with hepatic inflammation [25] and hepatocellular carcinoma [26]. Other molecules with reported oncogenic associations were also found in the highly-expressed, upregulated cluster and included *H19* [27], *SPARC* [28] and *SERPINE1* [29]. Furthermore, gene ontology (GO) over-representation analyses on all highly-expressed, upregulated genes revealed that the five most enriched and significant GO terms were tied to extracellular matrix genes associated with fibrosis and cirrhosis (p-values <0.0001), a hallmark of liver disease in A1ATD (Fig. 5G). This included collagen-related genes (e.g. *COL1A1*, *COL1A2*, *COL3A1*, *COL4A1* and *COL5A1*) and genes whose products are involved in the assembly and remodelling of the extracellular matrix such as ADAM

metallopeptidases (e.g. *ADAM19*), fibrillin (e.g. *FBN1*), fibronectin (e.g. *FN1*), laminins (e.g. *LAMB1*), thrombospondin (e.g. *THBS1*) and matrix-associated proteins encoded by *SPARC* and *WNT5A*. Taken together, these analyses uncovered highly relevant proteins involved in the response to *SERPINA1* mutations.

Validation of discoveries from the hiPSC-derived hepatocyte platform

We concluded that overall, several new areas of A1AT-deficient biology in HLCs were identified and warranted follow up. The most significant of which were: (1) A1AT polymers accumulated in a heterogenous manner within ZZ-HLC hepatocyte populations, (2) specific proteins associated with predisposition to malignancy were found to be highly upregulated in ZZ-HLCs, (3) mitochondrial biology in ZZ-HLCs was abnormally affected, and (4) ZZ-HLCs displayed activation of important inflammatory and unfolded protein response pathways. To validate the relevance of these findings, we next assessed the accumulation of A1AT polymers in liver tissue from individuals with PiZZ A1ATD [30] (Fig. 6A). While the majority of hepatocytes exhibited no polymer accumulation, those displaying characteristic A1AT inclusions were mainly located at the periphery of hepatic lobules, thereby validating the cell-to-cell heterogeneity of polymer formation observed in ZZ-HLCs (Fig. 2A). We next compared genes differentially expressed in HLCs (ZZ-HLCs vs RR-HLCs) and primary hepatocytes (PiZZ vs PiMM) and found 80 upregulated genes common to both datasets (Fig. 6B). One of these 80 genes (*AKR1B10*) had a related enzyme product (AKR1B1) present exclusively in the ER-enriched proteome dataset of ZZ-HLCs (Fig. 5B) and a $\log_2$-fold change of 3.6

and 3.8 in differential gene expression between ZZ/RR-HLCs and PiZZ/PiMM hepatocytes respectively. The clinical significance of this molecule was assessed by immunostaining paraffin-embedded liver sections from three patients with PiZZ whose clinical backgrounds (age, sex and severity of disease) matched that of the original hiPSC line donor. Samples stained positively for AKR1B10 in clusters of cells that were also positive for polymers of A1AT (Fig. 6C). Having demonstrated the potential clinical relevance of the data generated from our *in vitro* model for biomarker discovery, we next sought to explore physiological pathways that may be underpinning A1AT pathogenesis by focusing on GO terms associated with unfolded protein binding. Utilizing STRING v9.1, we surveyed known and predicted protein-protein interactions encoded by those genes upregulated with the highest confidence view (score = 0.900) in ZZ-HLCs. We found evidence of gene network clusters indicating inflammatory (e.g. *IL18*) and cellular stress responses, (e.g. calnexin (*CANX*), calreticulin (*CALR*), BiP/GRP78 (*HSPA5*), ERdj5 (*DNAJC10*), ERdj6 (*DNAJC3*), *DNAJB11*, GRP94 (*HSP90B1*) and GRP170 (*HYOU1*) (Supplementary Fig. 2). The differential gene expression profile of ZZ-HLCs not only appeared to mirror components of the A1AT-deficient pathology that have previously been identified (e.g. *CANX* and *CALR*), but also uncovered new genetic networks. Of particular interest were those genes linking misfolding-induced inflammatory responses to mitochondrial abnormalities since our electron microscopy studies demonstrated ZZ-HLC populations contained markedly abnormal mitochondrial phenotypes (Fig. 6D), as also previously described in human tissue and HLCs [31]. We sought to validate the importance of these genes by

examining differential gene expression at the nexus of inflammatory (*IL-18* and *CASP4*) and unfolded protein (*CANX* and *CALR*) clusters in a second hiPSC cell model of A1ATD derived from a different patient in a different laboratory [32]. All four genes were also found to be upregulated in PiZZ versus PiMM cells, suggesting their importance for future investigations (Supplementary Fig. 3). Taken together, these data demonstrated that the biomarkers and putative new mechanisms identified by our approach could be clinically relevant for a broad number of A1AT-deficient patients.

DISCUSSION:

Despite the classification of A1ATD as a monogenetic disease, the underlying molecular mechanisms causing liver pathology are poorly understood. hiPSCs offer an appealing model to interrogate such questions but have until now been hampered by concerns over whether *in vitro* signatures reflect the human disease. To address this, our study characterised the molecular and cellular signatures of ZZ-HLCs in comparison to human tissue. We first determined that, as in patients, only a subset (~40 %) of ZZ-HLCs contained A1AT polymers and that these polymers are contained within the ER but physically isolated from the rest of the ER lumen. Of note, Tafaleng et al. previously utilised ZZ-HLCs and ZZ liver samples to establish the presence of globular inclusions and dilated ER [12]. Our studies elaborate on these observations by using ZZ/RR-HLCs to provide real-time proof of physical ER fractionation and absent functional connection between abnormal ER structures. Importantly, our analyses of liver samples from patients with A1ATD also suggest that the disease could be regionalised as these globular

inclusions were mainly located in the lobule periphery. Thus, disease progression mechanisms could be associated with liver zonation. To further shed light on the molecular mechanisms governing this specific type of intracellular A1AT retention, we then compared genome-wide RNA-seq and ER-specific proteomic datasets of ZZ-HLCs versus RR-HLCs. The foremost misregulated pathways, both on a transcriptomic and proteomic level, were associated with known pathways of the misfolded protein response. In addition, our analyses also revealed novel molecular proteins and pathways important in chaperone function, inflammation, mitochondrial dysfunction and malignancy, which we validated in human tissue.

Despite the persistent molecular and functional similarities of HLCs with foetal hepatocytes [33], this work has shown the adequacy of ZZ-HLCs to replicate the molecular pathways of PiZZ hepatocytes. Their developmental immaturity offers the opportunity to study the emergence, early onset and progression of A1ATD, even at stages in which the disease is still asymptomatic in most patients [34]. A good example of this is the photobleaching assays (Fig. 3+4), which clearly demonstrated that ZZ-HLCs have significant loss of protein mobility, ER luminal communication and in some cases complete disruption of ER cisternae into isolated units. Whilst it has previously been demonstrated that even small deviations in protein diffusion rates can lead to biologically relevant changes [35], our observations offer a novel insight into the sub-cellular anatomy of how this occurs in A1ATD. Such understanding is likely to be of clinical significance since cells harbouring fragmented ER inclusions have been shown to be more prone to apoptotic cell death and rely on replacement by globule-devoid hepatocytes with enhanced cell division rates

[36] [37]. However, whether A1AT polymer sequestration into globules is a protective cellular response or signals a state of injury in this setting (or even both) [37] [38] is currently not known. Further *in vitro* studies, combined with human histological specimens and clinical data may allow us to deconstruct this problem by examining whether there is a link between the severity and number of ER inclusions, and an association between the severity and progression of liver disease. In a similarly important and clinically relevant manner, early identification of A1AT-deficient patients who are likely to progress to cancerous states represents an unmet but urgently required clinical challenge. Whilst AKR1B10 has been associated with hepatocellular carcinoma [39] [40], its co-localisation within cells containing polymers (Fig. 6C) suggests an association of this protein with A1ATD. The presence of AKR1B10 may therefore be a direct consequence of polymerised protein accumulation, characterising a sub-set of hepatocytes primed towards malignancy, making AKR1B10 a potential tissue biomarker for hepatocellular carcinoma risk stratification. Other proteins with known liver/cancer associations such as cysteine cathepsin family member CTSO [41] [42] were also identified in our ZZ-HLC cells and may similarly provide prognostic and mechanistic insights into why individuals with A1ATD are at increased risk of tumourigenicity [43].

Understanding molecular pathways linking the polymerisation of Z A1AT to hepatic disease is central to the design of future therapeutics. Our genome and proteome analyses (Fig. 5) identified differentially-regulated genes known to have an association with A1ATD (e.g. proteins of the ER-associated degradation machinery) as well as novel factors required to recognise and

bind mutant glycoproteins, retro-translocate them from the ER lumen to the cytosol and tag them for proteasomal degradation. With the reassurance provided by this biological baseline, we also identified molecules that could offer insights into the pathophysiology of disease using transcriptomics and proteomics. The twenty highest-expressed, differentially upregulated genes in ZZ-HLCs were all of mitochondrial origin and associated with tasks of meeting higher energy demands. This manifested as physical disruption of the mitochondria (Fig. 6D) which although described previously [44], is not yet comprehensively characterised with respect to its key molecular participants [45]. Our data provide new insight into the link between ER misfolding and mitochondrial disruption. Of particular interest, ER-stress response proteins ARMET (*MANF*) [46], OASIS (*CREB3L1*) [47], quality control chaperone proteins (*HSP90* [48], Calreticulin [49], Calnexin [50]) and pro-inflammatory chemokines, cytokines and receptors ("inflammasome") known to mediate cytotoxic stress and inflammation (IL-1, IL-18, Caspase-4, TNF,) [51] [52] were upregulated in ZZ-HLCs. Interestingly, of the five most highly upregulated genes in ZZ-HLCs reported by Wilson et al., *CASP4* and *CFH* also appeared in our list of 1675 significant genes differentially regulated between ZZ-HLCs and RR-HLCs (FDR < 5%) [32]. We therefore propose these targets, known also to mediate inter-organelle communication, as potentially being pivotal to disease and worthy of further research. Finally, this work also indicates that a more direct drug screening approach to target these novel pathways in A1ATD is merited.

REFERENCES:

1. Byth, B.C., G.D. Billingsley, and D.W. Cox, *Physical and genetic mapping of the serpin gene cluster at 14q32.1: allelic association and a unique haplotype associated with alpha 1-antitrypsin deficiency.* Am J Hum Genet, 1994. **55**(1): p. 126-33.
2. Morrison, H.M., S.C. Afford, and R.A. Stockley, *Inhibitory capacity of alpha 1 antitrypsin in lung secretions: variability and the effect of drugs.* Thorax, 1984. **39**(7): p. 510-6.
3. Luisetti, M. and N. Seersholm, *Alpha1-antitrypsin deficiency. 1: epidemiology of alpha1-antitrypsin deficiency.* Thorax, 2004. **59**(2): p. 164-9.
4. Haq, I., et al., *Deficiency Mutations of Alpha-1 Antitrypsin. Effects on Folding, Function, and Polymerization.* Am J Respir Cell Mol Biol, 2016. **54**(1): p. 71-80.
5. Duvoix, A., B.D. Roussel, and D.A. Lomas, *Molecular pathogenesis of alpha-1-antitrypsin deficiency.* Rev Mal Respir, 2014. **31**(10): p. 992-1002.
6. Laurell, C.B. and S. Eriksson, *The electrophoretic alpha1-globulin pattern of serum in alpha1-antitrypsin deficiency. 1963.* COPD, 2013. **10 Suppl 1**: p. 3-8.
7. Carlson, J.A., et al., *Accumulation of PiZ antitrypsin causes liver damage in transgenic mice.* J Clin Invest, 1989. **83**: p. 1183-1190.
8. Gosai, S.J., et al., *Automated high-content live animal drug screening using C. elegans expressing the aggregation prone serpin alpha1-antitrypsin Z.* PLoS One, 2010. **5**(11): p. e15460.

9. Ordonez, A., et al., *Endoplasmic reticulum polymers impair luminal protein mobility and sensitize to cellular stress in alpha1-antitrypsin deficiency.* Hepatology, 2013. **57**(5): p. 2049-60.

10. Takahashi, K. and S. Yamanaka, *Induction of pluripotent stem cells from mouse embryonic and adult fibroblast cultures by defined factors.* Cell, 2006. **126**: p. 663-676.

11. Rashid, S.T., et al., *Modeling inherited metabolic disorders of the liver using human induced pluripotent stem cells.* J Clin Invest, 2010. **120**(9): p. 3127-36.

12. Tafaleng, E.N., et al., *Induced pluripotent stem cells model personalized variations in liver disease resulting from alpha1-antitrypsin deficiency.* Hepatology, 2015. **62**(1): p. 147-57.

13. Yusa, K., et al., *Targeted gene correction of α1-antitrypsin deficiency in induced pluripotent stem cells.* Nature, 2011. **478**(7369): p. 391-394.

14. Hannan, N.R., et al., *Production of hepatocyte-like cells from human pluripotent stem cells.* Nat Protoc, 2013. **8**(2): p. 430-437.

15. Rouhani, F., et al., *Genetic background drives transcriptional variation in human induced pluripotent stem cells.* PLoS Genet, 2014. **10**(6): p. e1004432.

16. Baxter, M., et al., *Phenotypic and functional analyses show stem cell-derived hepatocyte-like cells better mimic fetal rather than adult hepatocytes.* J Hepatol, 2015. **62**(3): p. 581-9.

17. American Thoracic, S. and S. European Respiratory, *American Thoracic Society/European Respiratory Society statement: standards for the diagnosis and management of individuals with alpha-1*

antitrypsin deficiency. Am J Respir Crit Care Med, 2003. **168**(7): p. 818-900.

18. Snapp, E.L., N. Altan, and J. Lippincott-Schwartz, *Measuring protein mobility by photobleaching GFP chimeras in living cells.* Curr Protoc Cell Biol, 2003. **Chapter 21**: p. Unit 21 1.
19. Dickens, J.A., et al., *The endoplasmic reticulum remains functionally connected by vesicular transport after its fragmentation in cells expressing Z-alpha1-antitrypsin.* FASEB J, 2016.
20. Costantini, L.M., et al., *Assessing the tendency of fluorescent proteins to oligomerize under physiologic conditions.* Traffic, 2012. **13**(5): p. 643-9.
21. Lippincott-Schwartz, J., E. Snapp, and A. Kenworthy, *Studying protein dynamics in living cells.* Nat Rev Mol Cell Biol, 2001. **2**(6): p. 444-56.
22. Schmidt, B.Z. and D.H. Perlmutter, *Grp78, Grp94, and Grp170 interact with alpha1-antitrypsin mutants that are retained in the endoplasmic reticulum.* Am J Physiol Gastrointest Liver Physiol, 2005. **289**(3): p. G444-55.
23. Lawless, M.W., et al., *Activation of endoplasmic reticulum-specific stress responses associated with the conformational disease Z alpha 1-antitrypsin deficiency.* J Immunol, 2004. **172**(9): p. 5722-6.
24. Chambers, J.E. and S.J. Marciniak, *Cellular mechanisms of endoplasmic reticulum stress signaling in health and disease. 2. Protein misfolding and ER stress.* Am J Physiol Cell Physiol, 2014. **307**(8): p. C657-70.

25. Yeung, E.N., et al., *Fibrinogen production is enhanced in an in-vitro model of non-alcoholic fatty liver disease: an isolated risk factor for cardiovascular events?* Lipids Health Dis, 2015. **14**: p. 86.

26. Gao, H.J., et al., *Quantitative proteomic analysis for high-throughput screening of differential glycoproteins in hepatocellular carcinoma serum.* Cancer Biol Med, 2015. **12**(3): p. 246-54.

27. Matouk, I.J., et al., *The H19 non-coding RNA is essential for human tumor growth.* PLoS One, 2007. **2**(9): p. e845.

28. Deng, B., et al., *MiRNA-211 suppresses cell proliferation, migration and invasion by targeting SPARC in human hepatocellular carcinoma.* Sci Rep, 2016. **6**: p. 26679.

29. Divella, R., et al., *Influence of plasminogen activator inhibitor-1 (SERPINE1) 4G/5G polymorphism on circulating SERPINE-1 antigen expression in HCC associated with viral infection.* Cancer Genomics Proteomics, 2012. **9**(4): p. 193-8.

30. Miranda, E., et al., *A novel monoclonal antibody to characterize pathogenic polymers in liver disease associated with alpha1-antitrypsin deficiency.* Hepatology, 2010. **52**(3): p. 1078-88.

31. Teckman, J.H., et al., *Mitochondrial autophagy and injury in the liver in [alpha]1-antitrypsin deficiency.* Am J Physiol, 2004. **286**: p. G851-G862.

32. Wilson, A.A., et al., *Emergence of a stage-dependent human liver disease signature with directed differentiation of alpha-1 antitrypsin-deficient iPS cells.* Stem Cell Reports, 2015. **4**(5): p. 873-85.

33. Baxter, M., et al., *Phenotypic and functional analyses show stem cell-derived hepatocyte-like cells better mimic fetal rather than adult hepatocytes.* J Hepatol, 2014.

34. Sveger, T., *The natural history of liver disease in alpha 1-antitrypsin deficient children.* Acta Paediatr Scand, 1988. **77**(6): p. 847-51.

35. Snapp, E.L., et al., *Monitoring chaperone engagement of substrates in the endoplasmic reticulum of live cells.* Proc Natl Acad Sci U S A, 2006. **103**(17): p. 6536-41.

36. Lindblad, D., K. Blomenkamp, and J. Teckman, *Alpha-1-antitrypsin mutant Z protein content in individual hepatocytes correlates with cell death in a mouse model.* Hepatology, 2007. **46**: p. 1228-1235.

37. Granell, S. and G. Baldini, *Inclusion bodies and autophagosomes: are ER-derived protective organelles different than classical autophagosomes?* Autophagy, 2008. **4**(3): p. 375-7.

38. Smith, S.E., et al., *Activating transcription factor 6 limits intracellular accumulation of mutant alpha(1)-antitrypsin Z and mitochondrial damage in hepatoma cells.* J Biol Chem, 2011. **286**(48): p. 41563-77.

39. Laffin, B. and J.M. Petrash, *Expression of the Aldo-Ketoreductases AKR1B1 and AKR1B10 in Human Cancers.* Front Pharmacol, 2012. **3**: p. 104.

40. Jin, J., et al., *Aldo-keto Reductase Family 1 Member B 10 Mediates Liver Cancer Cell Proliferation through Sphingosine-1-Phosphate.* Sci Rep, 2016. **6**: p. 22746.

41. Jedeszko, C. and B.F. Sloane, *Cysteine cathepsins in human cancer.* Biol Chem, 2004. **385**(11): p. 1017-27.

42. Leto, G., et al., *Lysosomal cathepsins B and L and Stefin A blood levels in patients with hepatocellular carcinoma and/or liver cirrhosis: potential clinical implications.* Oncology, 1997. **54**(1): p. 79-83.

43. Eriksson, S., J. Carlson, and R. Velez, *Risk of cirrhosis and primary liver cancer in alpha 1-antitrypsin deficiency.* N Engl J Med, 1986. **314**(12): p. 736-9.

44. Perlmutter, D.H., *Liver injury in alpha1-antitrypsin deficiency: an aggregated protein induces mitochondrial injury.* J Clin Invest, 2002. **110**(11): p. 1579-83.

45. Teckman, J.H., et al., *Mitochondrial autophagy and injury in the liver in alpha 1-antitrypsin deficiency.* Am J Physiol Gastrointest Liver Physiol, 2004. **286**(5): p. G851-62.

46. Apostolou, A., et al., *Armet, a UPR-upregulated protein, inhibits cell proliferation and ER stress-induced cell death.* Exp Cell Res, 2008. **314**(13): p. 2454-67.

47. Kondo, S., et al., *OASIS, a CREB/ATF-family member, modulates UPR signalling in astrocytes.* Nat Cell Biol, 2005. **7**(2): p. 186-94.

48. Altieri, D.C., *Hsp90 regulation of mitochondrial protein folding: from organelle integrity to cellular homeostasis.* Cell Mol Life Sci, 2013. **70**(14): p. 2463-72.

49. Ramos, R.R., A.J. Swanson, and J. Bass, *Calreticulin and Hsp90 stabilize the human insulin receptor and promote its mobility in the endoplasmic reticulum.* Proc Natl Acad Sci U S A, 2007. **104**(25): p. 10470-5.

50. Cameron, P.H., et al., *Calnexin phosphorylation attenuates the release of partially misfolded alpha1-antitrypsin to the secretory pathway.* J Biol Chem, 2009. **284**(50): p. 34570-9.

51. Shimada, K., et al., *Oxidized mitochondrial DNA activates the NLRP3 inflammasome during apoptosis.* Immunity, 2012. **36**(3): p. 401-14.

52. Lazarou, M., *Keeping the immune system in check: a role for mitophagy.* Immunol Cell Biol, 2015. **93**(1): p. 3-10.

FIGURE LEGENDS:

Fig. 1. Validating a cellular platform suitable for in-depth disease characterisation. (A) qPCR analyses for the denoted genes in ZZ- (mutant, n=12) and RR- (corrected, n=12) HLCs vs. positive controls (plated and fresh, cryopreserved human primary hepatocytes, n=2-3). (B) DELFIA of secreted α_1-antitrypsin and albumin in ZZ- and RR-HLCs; n=3-9. (C) Immunostaining of ZZ and RR-HLCs for HNFα, α_1-antitrypsin or albumin. Scale bar: 100 µm. (D) Pulse-chase analysis: Radioactively-labelled, newly-synthesised protein was tracked from the intracellular (lysate) to extracellular space (supernatant) at 1h, 2h and 4h.

Fig. 2. ZZ-HLCs display heterogenous abnormal ER morphology. (A) ER marker GFP-KDEL shows the different types of abnormal ER morphologies observed in ZZ-HLCs vs RR-HLCs. (B) Quantification of each ER morphology.

Fig. 3. Fluorescence loss in photobleaching (FLIP) shows absence of intra-cellular exchanges between ER inclusions. (A) FLIP of ZZ- and RR-HLCs

transfected with KDEL-GFP: Pre-bleach fluorescence was determined before bleaching. Fluorescence was monitored within equidistant areas (stars) from the area of bleach (red box). Graphs show normalized FLIP plots with pre-bleach intensities set to 100 %. N=5. (B) FLIP of ZZ-HLCs with large inclusions transfected with CytERM. Graph shows normalised FLIP plot with pre-bleach intensities set to 100%. N=3. (C) 100 µm Z-tack image of ZZ-HLCs. Scale bars: 10 µm.

Fig. 4. Fluorescent recovery after photobleaching (FRAP) confirming decrease ER protein mobility in ZZ-HLCs. (A) KDEL-GFP transfected cells were exposed to a single bleaching event (white box). (B) Recovery of GFP fluorescence by way of diffusion into the bleached area was measured by tracking fluorescence within the bleached area. (C) Slope of the fluorescent recovery curve and the mobile fraction indicate a significantly lower degree of protein mobility and higher viscosity in ZZ-HLCs with inclusions. Statistical analysis by unpaired, parametric t-test: $p \leq 0.01$ (**), $p \leq 0.0001$ (****).

Fig. 5. Proteomic and RNA-seq analyses capture novel disease signatures. (A) Experimental process for proteomic analyses. (B) List of proteins identified in the ER proteome (green: present) and (red: absent) between ZZ- and RR-HLC. (C) MA plot shows $\log_2$ fold changes in gene expression between ZZ- and RR-HLCs over the mean of normalised counts. Significant genes with Benjamini-Hochberg FDR < 0.05 are shown in red. (D) 319 gene-protein pairs with differential abundances and gene expression were identified (blue, adjusted p-values > 0.05 in red). (E) Most differentially expressed gene/protein pairs

upregulated (top) or downregulated (bottom). Horizontal lines: parameter boundaries of log2-fold change thresholds > 2 and < -2. (F) Data clustering showed the FPKM-based genes upregulated in ZZ-HLCs mapped into four groups: very high, high, low or very low expression. (G) Enriched gene ontology (GO) terms (p-value < 0.05) obtained from BioMart for the analysis of genes upregulated in ZZ-HLCs.

Fig. 6. Clinical relevance of novel disease signatures. (A) Immunostaining of PiZZ patient liver tissue sections confirmed (green arrow) and absence (red arrow) of PAS-positive α_1-antitrypsin globules (counter stained with polymer specific 2C1 antibody). Scale bar: 10 µm. (B) 1675 differentially regulated genes identified by RNA-seq of ZZ vs. RR-HLCs were compared to the top 1675 genes with the lowest p-values obtained by RNA-seq of one PiZZ vs. PiMM primary tissue sample. 80 genes were shared between the two gene lists. (C) AKR1B10 immunostaining of liver sections (n=3 patients) with clinical backgrounds matching the original hIPSC donor's. Staining with the 2C1 antibody confirmed presence of polymer in same cells as AKR1B10; negative controls (secondary antibody alone). Scale bar: 20 µm. (D) Electron microscopy comparing mitochondria in ZZ vs. RR-HLCs. Organelles with highly compressed morphology yielding heterogeneous electron densities are indicated (red arrows). Scale bar: 2 µm.

Figure 1

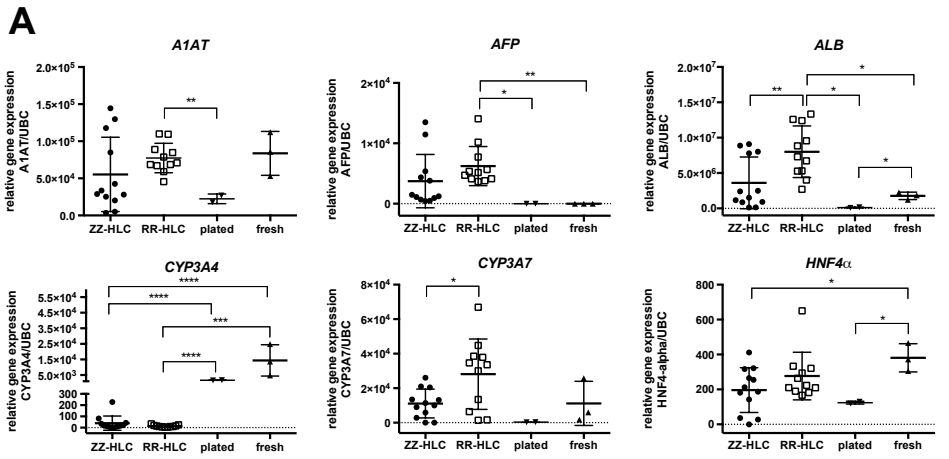
A
A1AT
AFP
ALB
CYP3A4
CYP3A7
HNF4α
relative gene expression A1AT/UBC
relative gene expression AFP/UBC
relative gene expression ALB/UBC
relative gene expression CYP3A4/UBC
relative gene expression CYP3A7/UBC
relative gene expression HNF4-alpha/UBC
ZZ-HLC
RR-HLC
plated
fresh

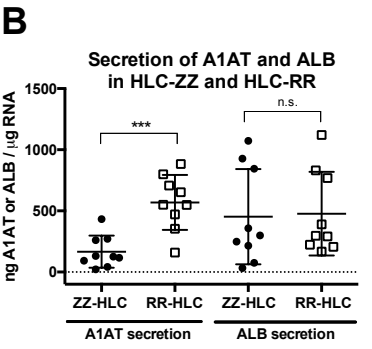
B
Secretion of A1AT and ALB in HLC-ZZ and HLC-RR
ng A1AT or ALB / µg RNA
n.s.
ZZ-HLC
RR-HLC
A1AT secretion
ALB secretion

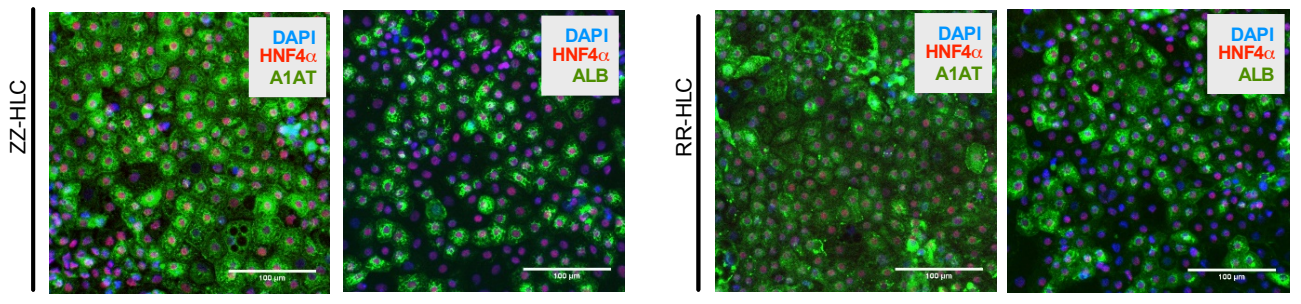
C
ZZ-HLC
RR-HLC
DAPI
HNF4α
A1AT
ALB
100 µm

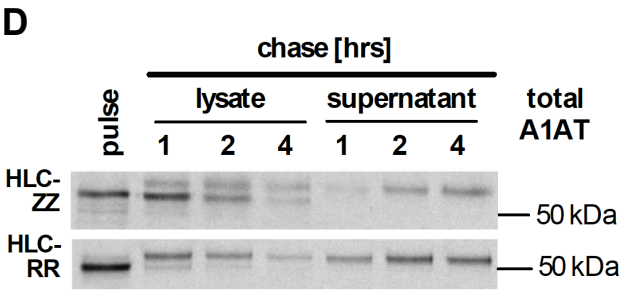
D
chase [hrs]
pulse
lysate
supernatant
total A1AT
1
2
4
HLC-ZZ
HLC-RR
50 kDa

Figure 2:

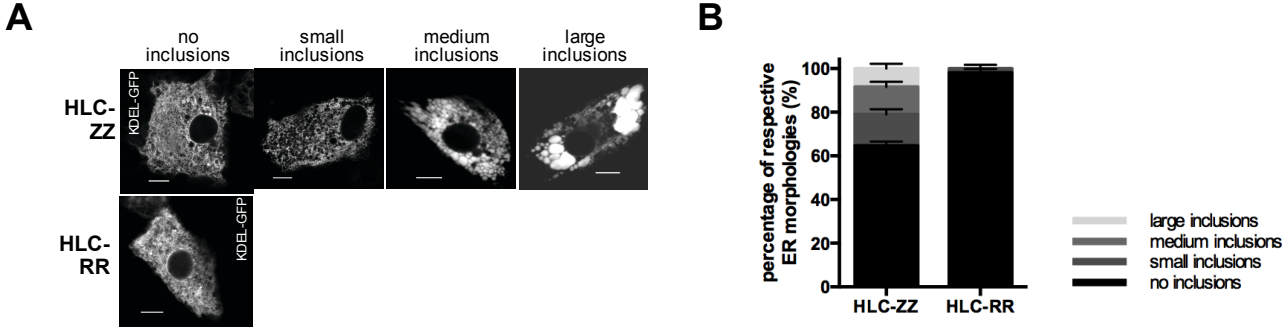
A
no inclusions
small inclusions
medium inclusions
large inclusions
HLC-ZZ
HLC-RR
KDEL-GFP
KDEL-GFP
B
percentage of respective ER morphologies (%)
100
80
60
40
20
0
HLC-ZZ
HLC-RR
large inclusions
medium inclusions
small inclusions
no inclusions

Figure 3:

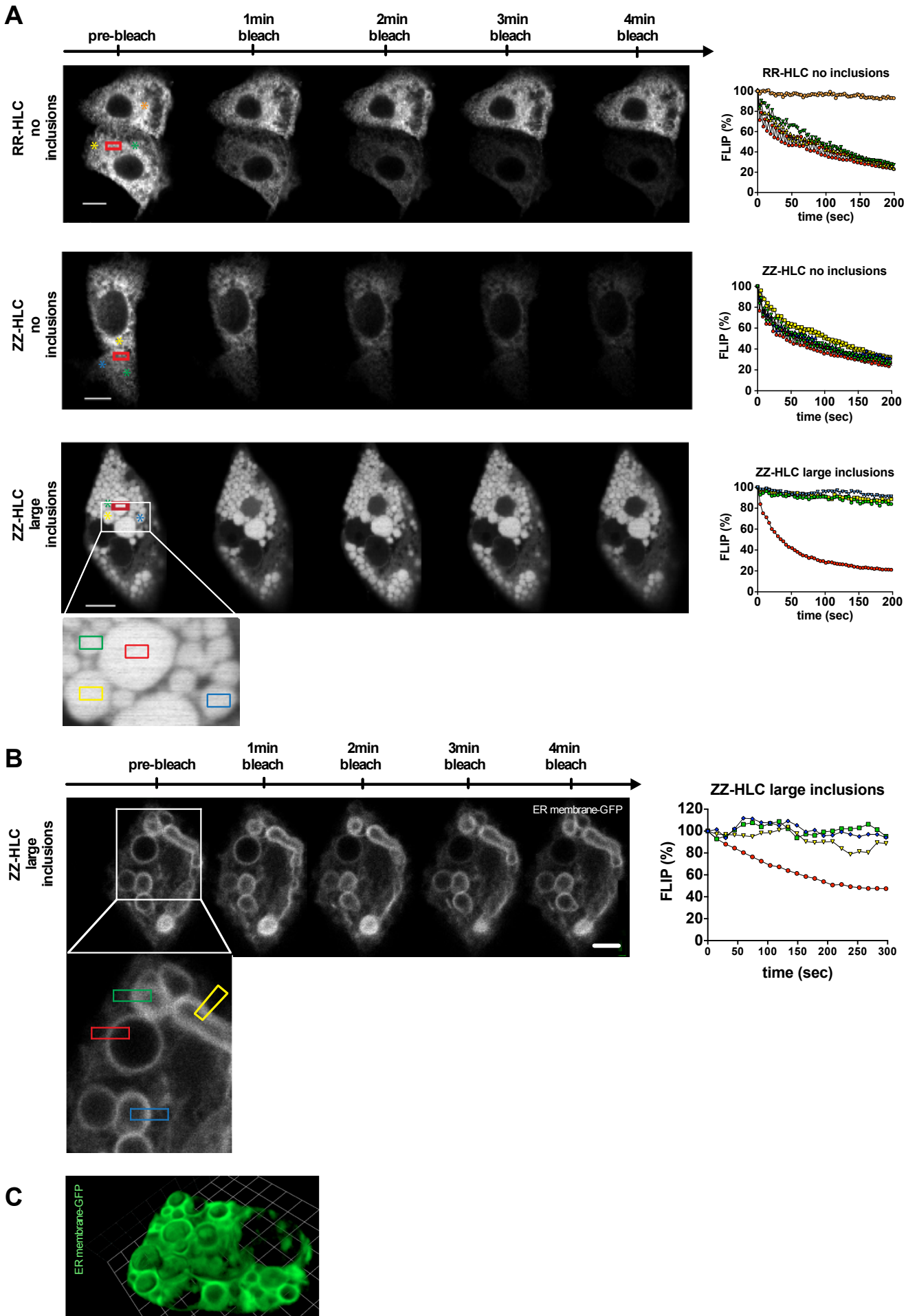
A
pre-bleach
1min bleach
2min bleach
3min bleach
4min bleach
RR-HLC no inclusions
ZZ-HLC no inclusions
ZZ-HLC large inclusions
RR-HLC no inclusions
ZZ-HLC no inclusions
ZZ-HLC large inclusions
FLIP (%)
time (sec)
B
pre-bleach
1min bleach
2min bleach
3min bleach
4min bleach
ZZ-HLC large inclusions
ER membrane-GFP
ZZ-HLC large inclusions
FLIP (%)
time (sec)
C
ER membrane-GFP

Figure 4:

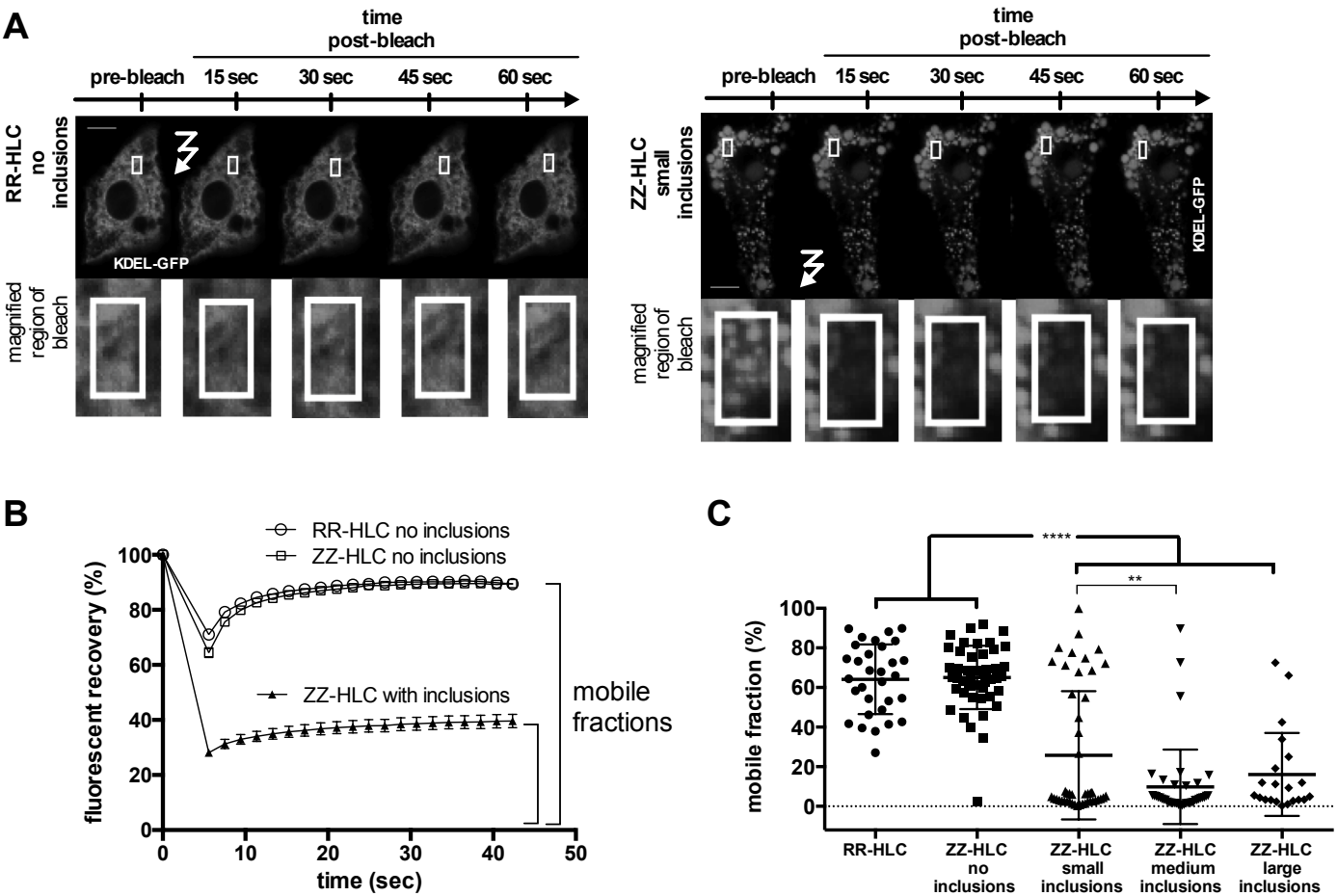
A
time
post-bleach
pre-bleach
15 sec
30 sec
45 sec
60 sec
RR-HLC
no
inclusions
KDEL-GFP
magnified
region of
bleach
ZZ-HLC
small
inclusions
KDEL-GFP
B
RR-HLC no inclusions
ZZ-HLC no inclusions
ZZ-HLC with inclusions
mobile
fractions
fluorescent recovery (%)
time (sec)
C
****
**
mobile fraction (%)
RR-HLC
ZZ-HLC
no
inclusions
ZZ-HLC
small
inclusions
ZZ-HLC
medium
inclusions
ZZ-HLC
large
inclusions

Figure 5:

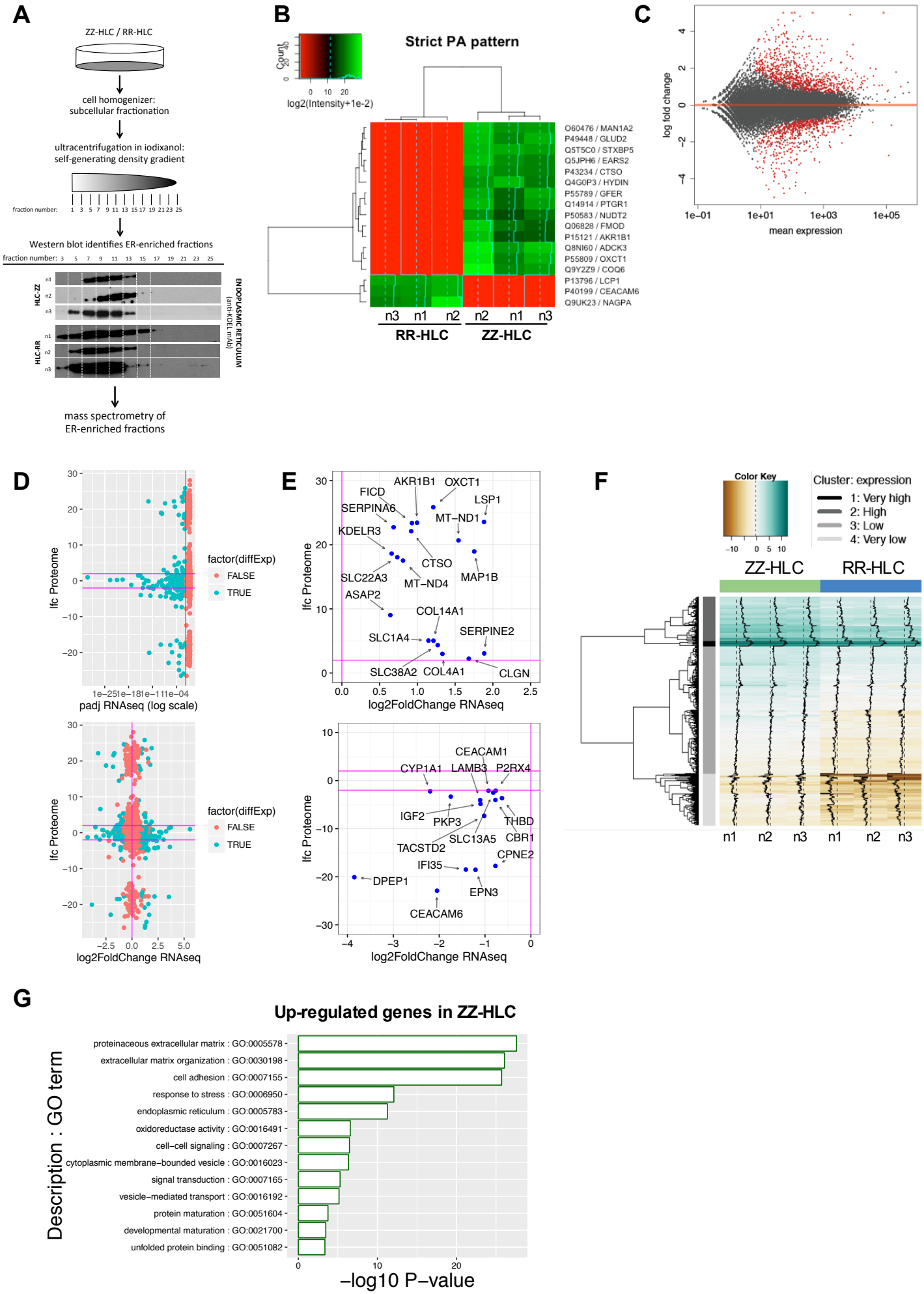
A
ZZ-HLC / RR-HLC
cell homogenizer:
subcellular fractionation
ultracentrifugation in iodixanol:
self-generating density gradient
fraction number:
Western blot identifies ER-enriched fractions
HLC-ZZ
HLC-RR
ENDOPLASMIC RETICULUM
(anti-KDEL mAb)
mass spectrometry of
ER-enriched fractions
B
Strict PA pattern
log2(Intensity+1e-2)
O60476 / MAN1A2
P49448 / GLUD2
Q5T5C0 / STXBP5
Q5JPH6 / EARS2
P43234 / CTSO
Q4G0P3 / HYDIN
P55789 / GFER
Q14914 / PTGR1
P50583 / NUDT2
Q06828 / FMOD
P15121 / AKR1B1
Q8NI60 / ADCK3
P55809 / OXCT1
Q9Y2Z9 / COQ6
P13796 / LCP1
P40199 / CEACAM6
Q9UK23 / NAGPA
RR-HLC
ZZ-HLC
C
log fold change
mean expression
D
lfc Proteome
padj RNAseq (log scale)
factor(diffExp)
FALSE
TRUE
log2FoldChange RNAseq
E
AKR1B1
OXCT1
FICD
LSP1
SERPINA6
MT−ND1
KDELR3
CTSO
SLC22A3
MT−ND4
MAP1B
ASAP2
COL14A1
SERPINE2
SLC1A4
SLC38A2
COL4A1
CLGN
CEACAM1
CYP1A1
LAMB3
P2RX4
IGF2
PKP3
THBD
SLC13A5
CBR1
TACSTD2
CPNE2
IFI35
DPEP1
EPN3
CEACAM6
F
Color Key
Cluster: expression
1: Very high
2: High
3: Low
4: Very low
ZZ-HLC
RR-HLC
n1
n2
n3
G
Up-regulated genes in ZZ-HLC
proteinaceous extracellular matrix : GO:0005578
extracellular matrix organization : GO:0030198
cell adhesion : GO:0007155
response to stress : GO:0006950
endoplasmic reticulum : GO:0005783
oxidoreductase activity : GO:0016491
cell−cell signaling : GO:0007267
cytoplasmic membrane−bounded vesicle : GO:0016023
signal transduction : GO:0007165
vesicle−mediated transport : GO:0016192
protein maturation : GO:0051604
developmental maturation : GO:0021700
unfolded protein binding : GO:0051082
Description : GO term
−log10 P−value

Figure 6:

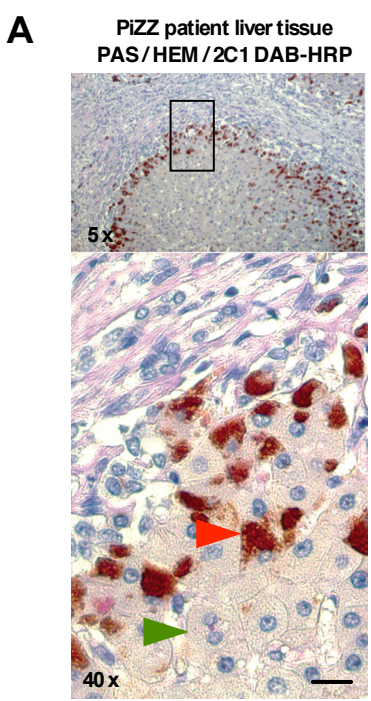

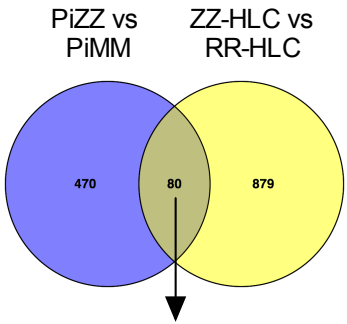

GO Biological Property Term	p-Value
GO:0009611~response to wounding	5.75E-09
GO:0051605~protein maturation by peptide bond cleavage	3.02E-08
GO:0016485~protein processing	1.89E-07
GO:0051604~protein maturation	3.40E-07
GO:0006956~complement activation	4.77E-07
GO:0002541~activation of plasma proteins involved in acute inflamma	5.38E-07
GO:0002526~acute inflammatory response	1.71E-06
GO:0006958~complement activation, classical pathway	3.97E-06
GO:0002455~humoral immune response mediated by circulating immı	5.23E-06
GO:0042060~wound healing	6.86E-06
GO:0006959~humoral immune response	1.14E-05
GO:0006954~inflammatory response	2.64E-05
GO:0002253~activation of immune response	2.66E-05
GO:0016064~immunoglobulin mediated immune response	4.93E-05
GO:0019724~B cell mediated immunity	5.69E-05

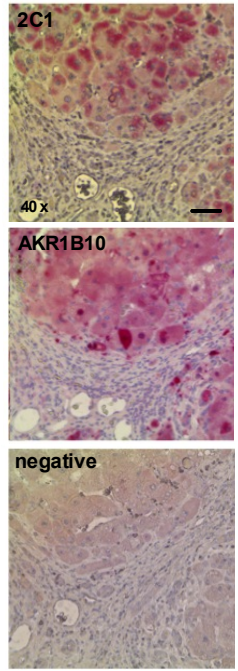

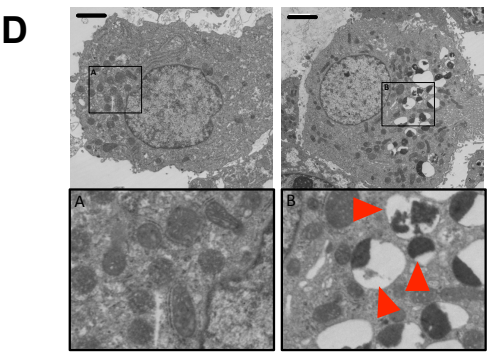

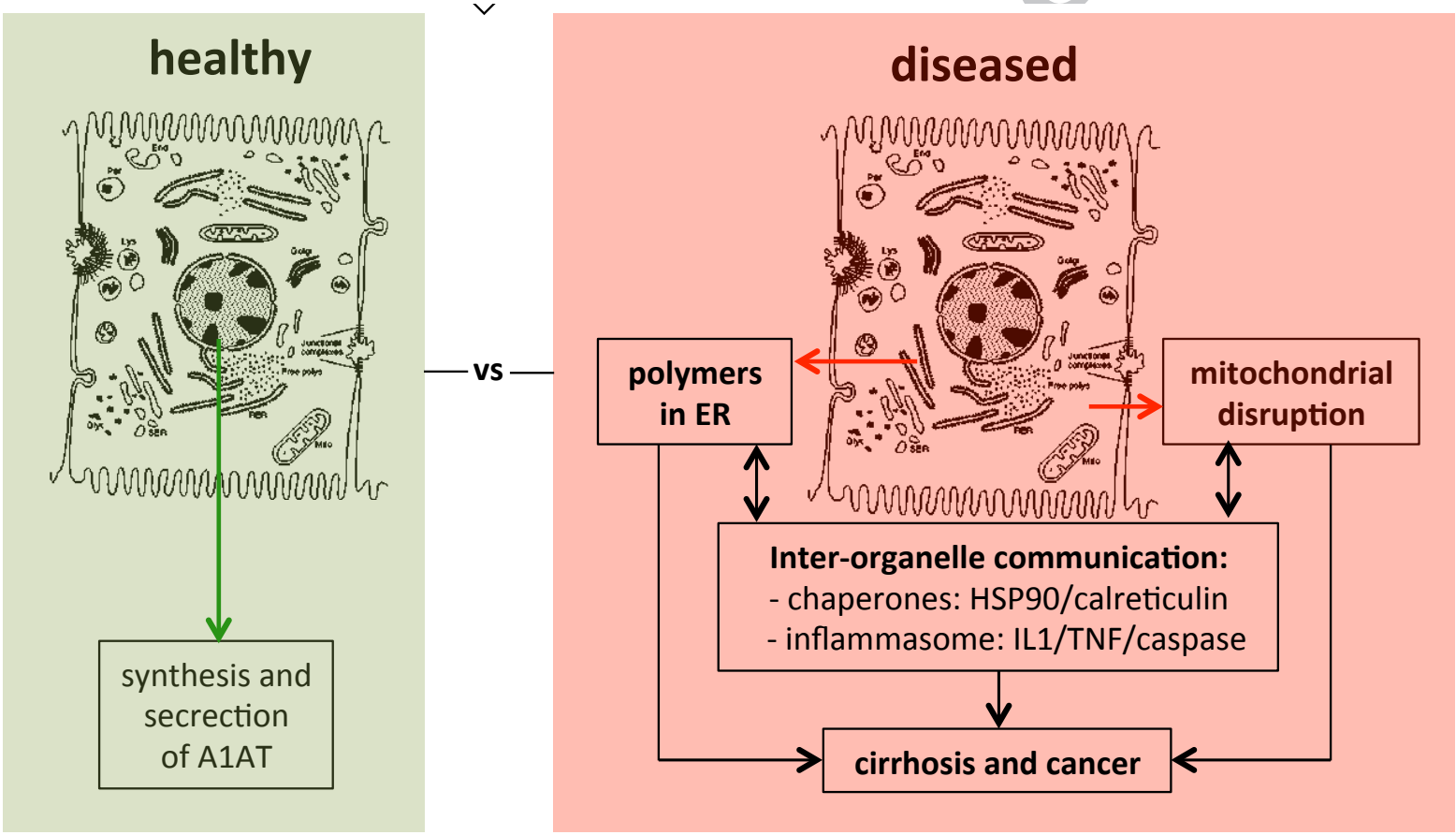

hiPSC hepatocyte model demonstrates the role of unfolded protein response and inflammatory networks in alpha1-antitrypsin deficiency

Ref: JHEPAT-D-17-01983

Charis-Patricia Segeritz et al.,

HIGHLIGHTS:

- Modelling α_1-antitrypsin deficiency liver disease using hiPSC-derived hepatocytes reveals disruption of the endoplasmic reticulum into isolated cisternae.
- Comparative transcriptomic and proteomics between diseased hiPSC-derived hepatocytes and their isogenic wildtype provides insights into disease mechanisms.
- AKR1B10 was identified as a putative biomarker for α_1-antitrypsin deficiency.